Dependence of Sheet Resistivity on Urbach Energy of Nano TiO_2 - Graphene-based Electrode for DSSC Application

Geoffrey Gitonga Riungu [1], **Simon Waweru Mugo** [1], **James Mbiyu Ngaruyia** [1], **Leonard Gitu** [1]

[1] *Jomo Kenyatta University of Agriculture and Technology*
P.O. Box 62000 – 00200 Nairobi, Kenya

DOI: 10.22178/pos.103-31

LCC Subject Category: QC1–999

Received 26.03.2024
Accepted 25.04.2024
Published online 30.04.2024

Corresponding Author:
Geoffrey Gitonga Riungu
geoffreyriungu@gmail.com

Abstract. The importance of renewable energy cannot be over-emphasized. Titanium IV oxide (TiO_2) is the most suitable semiconductor for dye-sensitized solar cells (DSSC) due to its chemical stability, non-toxicity and excellent optoelectronic properties. In this research, TiO_2 is coated on Graphene to enhance its charge transport, aiming to reduce recombination, a main setback in DSSCs. Understanding Graphene- TiO_2 contact is, therefore, essential for DSSC application. Using doctor blading, TiO2 thin films were deposited on single-layer graphene (SLG) and fluorine tin oxide (FTO). The films were annealed at 2 °C /min and 1 °C/min up to a temperature of 450 °C, then sintering at this temperature for 30 minutes. Four four-point probes SRM -232 were used to measure the samples' sheet resistance. The film thickness was obtained from transmittance using pointwise unconstrained minimization approximation (PUMA). UV–VIS spectrophotometer was employed to measure transmittance. The resistivity of TiO_2 on both FTO and Graphene was of order 10^{-4} Ω cm. However, TiO_2 annealed on graphene matrix exhibited a slightly lower resistivity, 5.6 x10^{-4} Ω cm, compared to 6.0 x10^{-4} Ω cm on FTO. Optical transmittance on the visible region was lower for TiO_2 on FTO than on SLG, 71.48% and 80.11%, respectively. The annealing rate decreased the weak absorption region's Urbach energy (Eu). Urbach energies for 1°C/min TiO_2 on FTO and SLG were 361 meV and 261 meV, respectively. This accounted for the decrease in film disorders due to annealing. A striking relation between sheet resistivity and Urbach was reported, suggesting SLG as a suitable candidate for the photoanode of a DSSC.

Keywords: Graphene; Urbach energy; Resistivity; Annealing; Titanium IV oxide.

INTRODUCTION

Dye-sensitized cells researchers have revolution is mainly based on titanium dioxide (TiO_2) films due to their excellent optoelectronic properties, such as high refractive index, large band gap and high transmittance in the visible region [1]. The optical and structural properties of TiO_2 films can be tailored to promote their applications via deposition methods such as sputtering, doctor blading, chemical vapour deposition, and sol-gel processes [2]. Doctor Blade is a popular approach because it is simple, easy to scale up, cost-effective and suitable for large-area processing [3]. Several studies have been initiated to modify the electrical transport properties of TiO_2 using binary-system electrodes [4].

Graphene-based devices are promising candidates for future high-speed field-effect transistors (FETs) because they have a high carrier mobility of more than $10^4 cm^2 V^{-1} s^{-1}$ [5]. The mono-layer Graphene is a zero-gap semiconductor with a linear dispersion. In contrast, the multilayer graphene is a semimetal with a small band overlap between the conduction and valence bands. Electrons through single-layer graphene hop with minimal scattering and at a very high Fermi velocity of $\sim 10^6 m/s$ [6].

The SRM-232 offers a low-cost hand-held sheet resistance meter with a four-point probe for measuring the sheet resistance of applied coatings such as conductive paints, EMI coatings, ITO on glass, and many other types of thin films.

Generally, near band edges in optical absorption, an electron from the top of the valence band gets excited into the bottom of the conduction band across the energy band gap [7]. The Urbach energy, indicating the width of the exponentially decaying sub-bandgap absorption tail, is commonly used to indicate the electronic quality of thin-film materials for application in solar cells [8].

This work analyses the electrical conductivity of TiO_2 grown on single-layer Graphene (SLG), and the relationship to Urbach energies is thus reported. This study aims to advance the optoelectronic applications of SLG to dye-sensitized solar cells.

Experimental procedure

Graphene. Single-layer Graphene was sourced from Charmgraphene Co. Ltd, Gwonseon-gu, Suwon, Republic of Korea. Graphene films were synthesized with thermal chemical vapour deposition (CVD) technology based on the roll-to-roll method. SLG was coated on a SiO_2 substrate.

TiO_2. Nanocrystalline TiO_2 (T/SP, 18% wt, sourced from Solaronix, Switzerland.

Fluorine-doped tin IV oxide (FTO). FTO (SnO_2: F) 7 Ω/sq, was sourced from Xinyan Technology Co. Limited, China.

Thin film deposition and annealing. Thin films were coated on FTO and SLG using the doctor blading technique. The prepared films were annealed using a muffle furnace at controlled rates of 1 °C/min and 2 °C/min from room temperature up to 450 °C. The films were then sintered for 30 minutes and cooled gradually back to room temperature.

Measurements and analysis

The optical transmittance was measured using a beam UV-visible spectrophotometer (Shimadzu UV probe 1800, Japan) in the 200-1100 nm wavelength range. Absorption coefficient Values for all corresponding wavelengths were obtained using SCOUT thin film analysis software [9]. The sheet resistance of the films was measured using a four-point probe, model SRM-232, as shown in Figure 1.

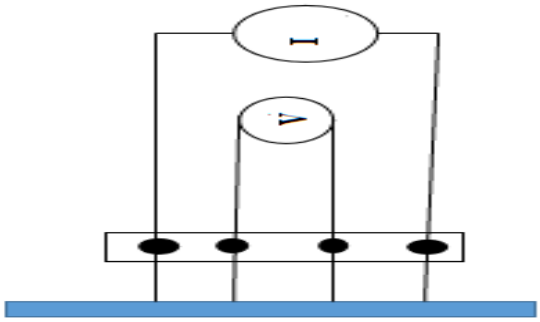

Figure 1 – Functional block diagram of SRM-232 Four-point probe

The voltage was measured across the inner probes, while the current was measured across the outer probes. The probes were operated manually by pressing the film. Sheet resistance (R_S) values are calculated and displayed on the digital panel. Resistivity (ρ) is defined in terms of voltage (V), current (I) and thickness (t) as in Equations 1 and 2.

$$\rho = 4.532 \frac{V}{I} t \quad (1)$$

$$\rho = 4.532 R_s\, t\ (\Omega\text{cm}) \quad (2)$$

The Urbach energy was calculated by plotting ln(α) vs hν and fitting the linear part of the curve with a straight line. The gradient of the line was used to calculate the search energies [10] as in Equation 3.

$$\alpha(h\nu) = \alpha_0 exp(\frac{h\nu}{E_u}) \quad (3)$$

A pointwise unconstrained optimization approach (PUMA) was used to estimate the thickness of the films from transmittance data [11]. Fora thin film deposited on a thick transparent substrate. The formulae giving thickness of film from the transmittance as a function of the wavelength λ is derived as shown [12] from Equations 4-9:

$$\text{Transmittance (T)} = \frac{Ax}{B - Cx + Dx^2} \quad (4)$$

$$\text{where } A = 16s(n^2 + \kappa^2) \quad (5)$$

$$B = [(n+1)^2 + \kappa^2] \; [(n+1)(n+s^2) + \kappa^2] \quad (6)$$

$$C = [(n^2 - 1 + \kappa^2)(n^2 - s^2 + \kappa^2) - 2\kappa^2(s^2+1)]2\cos\phi - \kappa[2(n^2 - s^2 + \kappa^2) + (s^2+1)(n^2 - 1 + \kappa^2)]2\sin\phi \quad (7)$$

$$D = [(n-1)^2 + \kappa^2] \; (n-1)(n-s^2) + \kappa^2] \quad (8)$$

$$\phi = 4\pi nd/\lambda,\ x = \exp(-\alpha d),\ \alpha = 4\pi\kappa/\lambda. \quad (9)$$

where *d* is the thickness of the film, s and n are the substrate and film's refraction index, α is the absorption coefficient, and κ is the (dimensionless) extinction coefficient.

RESULTS AND DISCUSSION

Sheet resistance. Figure 2 shows sheet resistance for annealed TiO_2 on fluorine-doped tin IV oxide (FTO) and single-layer *G*raphene (SLG).

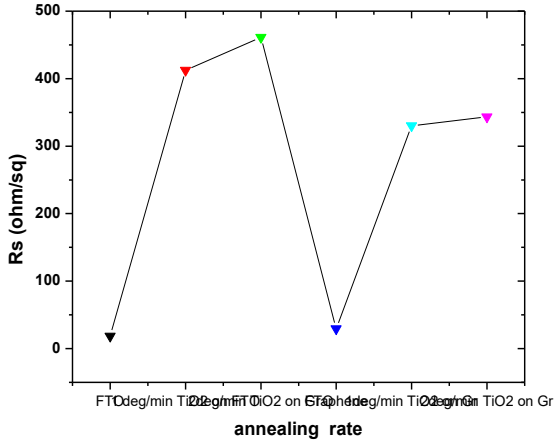

Figure 2 – Sheet resistance for annealed TiO2 on FTO and Graphene films

The *s*heet resistance of FTO is lower than SLG, 14.94798 and 31.62315 Ω/sq, respectively. However, TiO_2 annealed on graphene substrate exhibited lower resistance than on FTO substrate, 3.28 x10^2 and 4.12 x 10^2 Ω/sq, respectively. Mono-layer *G*raphene, through its planar hexagonal lattice structure, increases the layer conductivity for annealed TiO2, resulting in better electron transport for the composite film.

Sheet resistivity. Figure 3 shows the sheet resistivity of TiO_2 as a function of annealing and *the* effects of *G*raphene on the resistivity.

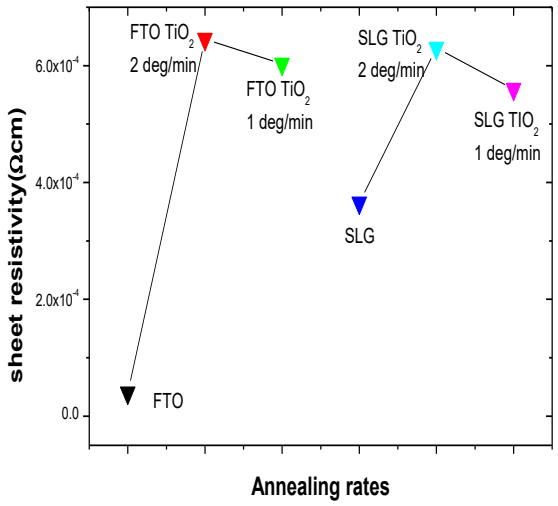

Figure 3 – Sheet resistivity against annealing for TiO2 on FTO and Graphene

The sheet resistivity of TiO_2 on both FTO and Graphene was of order 10^{-4} Ωcm. However, upon annealing TiO_2 at 1 °C per minute on the SLG sheet, resistivity is lower than on FTO. 5.6 x10^{-4} Ωcm is thus reported for SLG as compared to 6.0x10^{-4} Ωcm on FTO. FTO has uneven morphology, which results in high porosity of the TiO_2 layer, consequently producing subsurface defects in the FTO/TiO_2 interface. On the other hand, Graphene is highly crystalline. Therefore, this reduction in resistivity for TiO_2 annealed on Graphene could be attributed to better charge transport due to decreased lattice defects for TiO_2 annealed on Graphene.

Transmittance. Figure 4 shows transmittance spectra for tio2 annealed on FTO and SLG. Graphene on glass had a transmittance peak at a wavelength of 502.89 nm and 81.62%. Conversely, FTO peaked at 746.43 nm and 80.28% transmittance, as shown in Table 1.

For the annealed TiO_2, the peaks were at 686.71 nm and 754.22 nm for SLG and FTO, respectively. Transmittance for annealed films decreased more for FTO than Graphene at 66.25% and 71.95%, respectively.

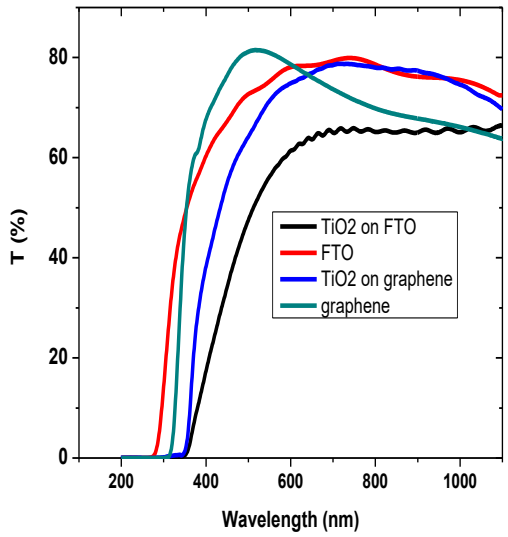

Figure 4 – Transmittance for annealed TiO2 on Graphene and FTO versus wavelength

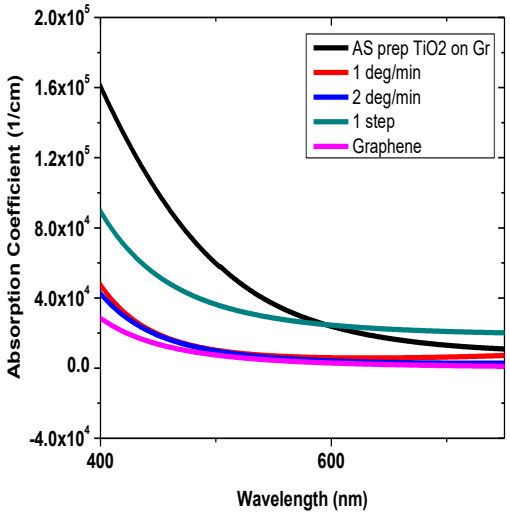

Figure 5 – Absorption coefficient for deposited and annealed TiO2 films on Graphene

High transmittance means that very few bonds of TiO_2 absorb a particular wavelength. Low transmittance implies a high number of TiO_2 bonds corresponding to vibrational energies of the incident wavelength. Thus, there is more absorption for TiO_2 on FTO than on Graphene. The peaks shift deeper in the visible region due to annealing, as shown in Table 1.

Table 1 – Transmittance peaks for TiO2 annealed on FTO and Graphene

Sample	Peak wavelength (λ) (nm)	Peak Transmittance (%)
Graphene	502.89	81.62
TiO_2 on Graphene	686.71	71.95
FTO	746.43	80.28
TiO_2 on FTO	754.22	66.25

Absorption coefficient. A graph of absorption coefficients against wavelength is shown in Figure 5. The absorption is of order 10^4 for all samples.

The coefficients decrease exponentially for all samples within the visible region. This indicates the presence of localized states in the band gap. The absorption edge can be used to measure the energy bandgap. The absorption coefficient's dependence was used to evaluate Urbach energies using the Urbach rule as in Equation 3.

Urbach energy for TiO_2 on Graphene and FTO. Figure 6 shows the dependence of absorption coefficient edges tailing in weak absorption region (W) and Urbach region (U) optical transitions from the extended state (T). Tailing of ρ(hν) extending into the energy band gap in region W is observed for TiO_2 on Graphene and FTO. The tailing is more pronounced for TiO_2 on FTO than on Graphene.

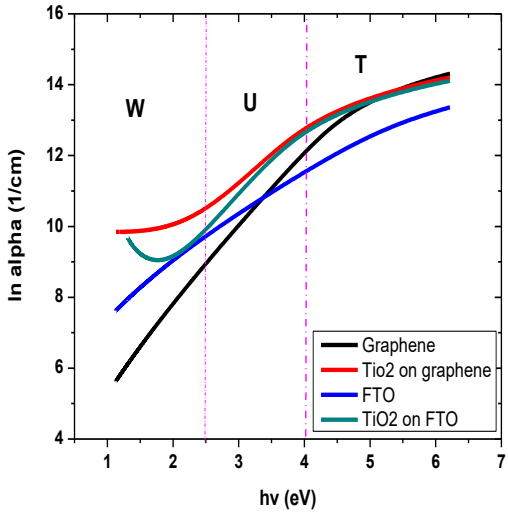

Figure 6 – ln (α) vs (hυ) for annealed TiO2 on Graphene and FTO

Exponential tails are associated with low crystalline films and disordered amorphous materials

because of localized states [13, 14]. Further, band tailing is associated with lattice vibration due to the creation of sub-surface defects such as vacancy-interstitial pairs and antisites [15]. Therefore, this tailing implies the presence of more localized states in the band gap for TiO_2 coated on FTO than on Graphene. The absence of tailing for Graphene and FTO signifies minimal or no localized states. To quantify the broadness of the density of states, Ubarch energies were evaluated using Equation 3. The Urbach Energy enumerates the steepness of the absorption onset near the band edge.

The evaluated Urbach energies of TiO2 films on FTO were higher than those of SLG, as shown in Table 2. High Urbach energy confirms enhanced photocatalytic efficiency due to the disorder and defects that introduced localized states at or near the conduction band level [16]. Therefore, lower Urbach energies of 260 meV signify fewer lattice defects for TiO_2 on the SLG substrate.

Table 2 – Urbach energies of TiO2 on FTO and Graphene

Urbach energy	2º/ min	1º/min
Tio_2 on FTO Eu (meV)	414	365
TiO_2 on Graphene(meV)	329	260

Relationship of Urbach energy and resistivity of TiO_2 on Graphene and FTO. In Figure 7, we observe a direct variation between Urbach energy and sheet resistivity of TiO2 on FTO and SLG. The optical band gap, Urbach energy, and electrical resistivity were found to depend systematically on the crystallite size [17]. In low crystalline, weakly crystalline, disordered, and amorphous materials, an exponential tail, known as the Urbach tail, exists at the band edge of the absorption/absorption coefficient curve. This exponential tail plays a crucial role in understanding the electronic transport properties of composite materials [18].

Therefore, as observed in Figure 7, TiO_2 annealed films on Graphene have a lower Urbach energy and sheet resistivity of 260 meV and 5.6 $x10^{-4}$ Ωcm. Annealing gradually increases crystallite sizes, decreases lattice imperfections, and enhances nucleation and coalescence.

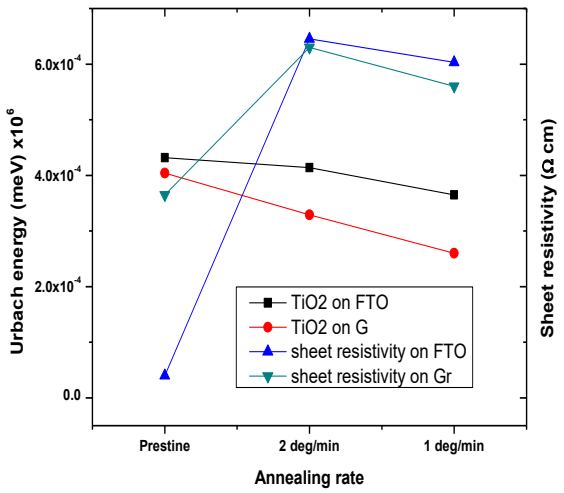

Figure 7 – A relation between Urbach energies and resistivity for TiO2 on FTO and Graphene

However, studies by [19] have reported that localized tail states in amorphous semiconductors arise from defects-generated disorder. The decrease in resistivity of TiO_2 on SLG can be attributed to the excellent conductivity of Graphene.

CONCLUSIONS

Uniform TiO_2 nanocomposite thin films were deposited on FTO and graphene interface glass substrates using the doctor-blading deposition technique. The four-point probe, model SRM-232, was used to measure the sheet resistance of the films. Sub-surface defects of the TiO_2 films on FTO and SLG, as manifested by the Urbach energy tails in the bandgap, were used to measure the disorder of the movie. A direct relation between Urbach energy and sheet resistivity as a result of annealing is thus reported for both TiO_2 on FTO and on Graphene. These observations indicate that fine control over sheet resistivity and microstructure of the films can be achieved via annealing TiO_2 on Graphene to harness it for various optoelectronic applications.

REFERENCES

1. Fuyuki, T., & Matsunami, H. (1986). Electronic Properties of the Interface between Si and TiO2 Deposited at Very Low Temperatures. *Japanese Journal of Applied Physics, 25*(9R), 1288. doi: 10.1143/jjap.25.1288

2. Miao, L., Jin, P., Kaneko, K., Terai, A., Nabatova-Gabain, N., & Tanemura, S. (2003). Preparation and characterization of polycrystalline anatase and rutile TiO2 thin films by rf magnetron sputtering. *Applied Surface Science*, 212–213, 255–263. doi: 10.1016/s0169-4332(03)00106-5

3. Benjamin, M., Simon, W., & James, M. (2018). Effect of Annealing Rates on Surface Roughness of TiO_2 Thin films. *Journal of Materials Physics and Chemistry, 6*(2), 43–46.

4. Jose, R., Thavasi, V., & Ramakrishna, S. (2009). Metal Oxides for Dye-Sensitized Solar Cells. *Journal of the American Ceramic Society, 92*(2), 289–301. doi: 10.1111/j.1551-2916.2008.02870.x

5. Geim, A. K., & Novoselov, K. S. (2007). The rise of Graphene. *Nature Materials, 6*(3), 183–191. doi: 10.1038/nmat1849

6. Novoselov, K. S., Geim, A. K., Morozov, S. V., Jiang, D., Zhang, Y., Dubonos, S. V., Grigorieva, I. V., & Firsov, A. A. (2004). Electric Field Effect in Atomically Thin Carbon Films. *Science, 306*(5696), 666–669. doi: 10.1126/science.1102896

7. Boubaker, K. (2011). A physical explanation to the controversial Urbach tailing universality. *The European Physical Journal Plus, 126*(1). doi: 10.1140/epjp/i2011-11010-4

8. Subedi, B., Li, C., Chen, C., Liu, D., Junda, M. M., Song, Z., Yan, Y., & Podraza, N. J. (2022). Urbach Energy and Open-Circuit Voltage Deficit for Mixed Anion–Cation Perovskite Solar Cells. *ACS Applied Materials & Interfaces, 14*(6), 7796–7804. doi: 10.1021/acsami.1c19122

9. Theiss, W. (2008). *Scout*. Retrieved from https://www.wtheiss.com/download/scout3.pdf

10. Boubaker, K. (2011). A physical explanation to the controversial Urbach tailing universality. *The European Physical Journal Plus, 126*(1). doi: 10.1140/epjp/i2011-11010-4

11. Birgin, E. G., Chambouleyron, I. E., Martínez, J. M., & Ventura, S. D. (2003). Estimation of optical parameters of very thin films. *Applied Numerical Mathematics, 47*(2), 109–119. doi: 10.1016/s0168-9274(03)00055-2

12. Birgin, E. G., Chambouleyron, I., & Martínez, J. M. (1999). Estimation of the Optical Constants and the Thickness of Thin Films Using Unconstrained Optimization. *Journal of Computational Physics, 151*(2), 862–880. doi: 10.1006/jcph.1999.6224

13. El-Nahass, M. M., Soliman, H. S., & El-Denglawey, A. (2016). Absorption edge shift, optical conductivity, and energy loss function of nano thermal-evaporated N-type anatase TiO2 films. *Applied Physics A, 122*(8). doi: 10.1007/s00339-016-0302-6

14. Mathews, N. R., Morales, E. R., Cortés-Jacome, M. A., & Toledo Antonio, J. A. (2009). TiO2 thin films – Influence of annealing temperature on structural, optical and photocatalytic properties. *Solar Energy, 83*(9), 1499–1508. doi: 10.1016/j.solener.2009.04.008

15. Wibowo, K. M., Sahdan, M. Z., Asmah, M. T., Saim, H., Adriyanto, F., Suyitno, & Hadi, S. (2017). Influence of Annealing Temperature on Surface Morphological and Electrical Properties of Aluminum Thin Film on Glass Substrate by Vacuum Thermal Evaporator. *IOP Conference Series: Materials Science and Engineering, 226*, 012180. doi: 10.1088/1757-899x/226/1/012180

16. Jayasinghe, L., Jayaweera, V., de Silva, N., & Mubarak, A. M. (2022). Role of ZrO2 in TiO2 composites with rGO as an electron mediator to enhance the photocatalytic activity for the photodegradation of methylene blue. *Materials Advances, 3*(21), 7904–7917. doi: 10.1039/d2ma00754a

17. Ali, D., Butt, M. Z., Muneer, I., Bashir, F., & Saleem, M. (2017). Correlation between structural and optoelectronic properties of tin doped indium oxide thin films. *Optik, 128*, 235–246. doi: 10.1016/j.ijleo.2016.10.028

18. Rahman, Md. (2023). Synthesis of CdS and CdTe Through A Novel Solution Process for Application in Thin Film Solar Cells. Retrieved from https://www.researchgate.net/publication/373603736

19. Al-Shomara, S. M., & Alahmad, W.R. (2019). Annealing temperature effect on structural, optical and photocatalytic activity of nanocrystalline tio2films prepared by sol-gel method used for solar cell application. *Digest Journal of Nanomaterials and Biostructures, 14*(3), 617–625.